Structural Engineering and Mechanics, Vol. 45, No.4 (2013) 439-454
DOI: http://dx.doi.org/10.12989/sem.2013.45.4.439

Design and homogenization of metal sandwich tubes with prismatic cores

Kai Zhang[1,3], Zichen Deng[*1,2], Huajiang Ouyang[3] and Jiaxi Zhou[4]

[1]*School of Mechanics, Civil Engineering and Architecture, Northwestern Polytechnical University, Xi'an 710072, China*
[2]*State Key Laboratory of Structural Analysis for Industrial Equipment, Dalian University of Technology, Dalian 116024, China*
[3]*School of Engineering, University of Liverpool, Liverpool L69 3GH, United Kingdom*
[4]*College of Mechanical and Vehicle Engineering, Hunan University, Changsha 410082, China*

(Received September 9, 2011, Revised December 11, 2012, Accepted January 3, 2013)

Abstract. Hollow cylindrical tubes with a prismatic sandwich lining designed to replace the solid cross-sections are studied in this paper. The sections are divided by a number of revolving periodic unit cells and three topologies of unit cells (Square, Triangle and Kagome) are proposed. Some types of multiple-topology designed materials are also studied. The feasibility and accuracy of a homogenization method for obtaining the equivalent parameters are investigated. As the curved elements of a unit cell are represented by straight elements in the method and the ratios of the lengths of the curved elements to the lengths of the straight elements vary with the changing number of unit cells, some errors may be introduced. The frequencies of the first five modes and responses of the complete and equivalent models under an internal static pressure and an internal step pressure are compared for investigating the scope of applications of the method. The lower bounds and upper bounds of the number of Square, Triangular and Kagome cells in the sections are obtained. It is shown that treating the multiple-topology designed materials as a separate-layer structure is more accurate than treating the structure as a whole.

Keywords: sandwich tube; homogenization method; prismatic core; multiple-topology designed materials

1. Introduction

Hollow cylindrical structures are an important kind of structures used in engineering and they usually experience complex loading and have complicated boundary conditions. For example, an engine combustor is subjected to internal pressures and high working temperature. A Pulse Detonation Engine (PDE) produces a huge amount of power and operates at subsonic up to supersonic speeds by a successive detonation waves produced in a combustor which is a typical hollow cylindrical structure.

*Corresponding author, Professor, E-mail: dweifan@nwpu.edu.cn

The fundamental mechanisms of the detonation propagation have been extensively studied (Cooper 2004, Shepherd 2005), while the design of the combustor is rarely studied. Because of a big pressure and a high temperature inside a Pulse Detonation Engine, the structural design of the tube is very important and there is a large scope for much innovation to achieve a high loading capacity, active heat dissipation capability and some other desirable combined properties. One design is to replace the solid tube with a prismatic core of cellular materials (Fig. 1) to suit the working environment through designing and optimizing the dimensions of the core element.

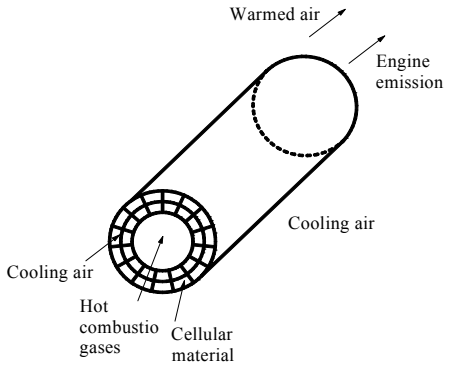

Fig. 1 PDE with cellular materials

Cellular materials have several advantages over monolithic solids, such as light weight, high specific strength, active heat dissipation potential and other attractive multi-functional characteristics (Evans *et al*. 2001, Fleck *et al*. 2010, Gibson and Ashby 1997). It is well known that cellular materials with prismatic cores are weight-efficient structures (Valdevit *et al*. 2004, Valdevit *et al*. 2006). Moreover, structures with an open cell topology which have the capability of active heat dissipation can be used as an active cooling panel (Gu *et al*. 2001, Lu *et al*. 2005, Valdevit *et al*. 2008). Considering the combined properties of cellular materials and various applications, designing a suitable structure which satisfies the requirement of load-bearing capability, high heat dissipation flux and others simultaneously via optimizations of the cell-wall thickness and length or cell topology (shape) is an active area of research (Evans *et al*. 2001, Kumar and McDowell 2009, Liu *et al*. 2007a, b, Seepersad *et al*. 2008).

A proper plate or shell model is required for the efficient design and the optimization of cellular structures. However, such models have a very large number of degrees-of-freedom. It is very useful to use homogenization models with equivalent parameters in analysis as the number of degrees of freedom required would be considerably smaller. Moreover, the responses of equivalent model (EM) with homogenization parameters can be calculated by using the mature classic shell theory. Therefore, it is important to find a proper method for obtaining the equivalent parameters and to verify the feasibility of the method. Many homogenization methods have been studied for cellular materials. A homogenization method for grid structures with triangular, hexagonal and quadrilateral cores was established by Hohe and Becker (Hohe and Becker 1999, 2001, Hohe *et al*. 1999). This method was based on the assumption that the strain energy stored in both the real microstructure and the homogenized model is equivalent and a displacement field was introduced

and equivalent structures with negative Poisson's ratios were derived in their research. A homogenization theory of finite deformation was established to analyze the microscopic symmetric bifurcation buckling of cellular solids subjected to macroscopically uniform compression by Ohno (Ohno *et al*. 2002). Based on the micro-polar theory, another homogenization method was put forward to get a continuum representation for two-dimensional periodic cellular solids (Kumar and McDowell 2004). The energy approach for square, equilateral triangular, mixed triangular and diamond cell topologies was used to obtain the linear elastic micro-polar constants. Then the effectiveness of this method was verified by a series of comparisons between the continuum representation and the exact discrete simulations of the cell structures under a point force. An effective computational model was obtained to predict the structural behaviour of lightweight sandwich panels having two-dimensional prismatic or three-dimensional truss cores by Liu (Liu *et al*. 2007c). This homogenization method was developed to obtain the homogenized macroscopic stiffness properties of the cellular core. The magnitude of errors between the homogenized model and the real sandwich panels was acceptable, but was not so small for non-orthotropic 3D truss cores.

Although there are many investigations about sandwich plate structures, investigations on the cylindrical sandwich structures are rare. A homogenization approach was put forward for obtaining the homogenised model of prismatic metal sandwich tubes with an internal moving pressure (Zhou *et al*. 2009). The small-strain kinematic analysis and the displacement field were introduced in that paper. The models with a 32 divisional revolving parts were calculated and the results demonstrated that the structural response and the maximum amplification factors of the complete model (CM) were similar to those of the equivalent model. It was assumed that the nodal points were connected with straight lines in that paper. Therefore, some errors may be introduced as the nodal points of the complete models are connected with arcs actually. The feasibility of that method should be studied though a series of calculations and comparisons and the scope of applications of that method should be ascertained for optimizations of the structures in future work.

In this paper, the homogenization method put forward by Liu *et al*. (2007c) and Zhou *et al*. (2009) used for calculating the homogenized parameters of the sandwich plates and cylindrical structures is adapted for calculating the homogenized parameters of the sandwich core of CM with different periodically divided unit cells and topologies. The responses of CM and EM under static and step pressures and the frequencies of the first five modes of these models are calculated. By comparing the results and analysing the errors, the applicability of this method for optimization of cylindrical sandwich structures can be assessed. Some types of multiple-topology designed materials which may have better performance in loading capacity, active heat dispassion and the multi-functional capability are studied in the last part of this paper.

2. Various core designs and the homogenization method

In the present study, CM is a hollow cylindrical tube with sandwich cross-sections and the cross-sections are equally divided by revolving periodic unit cells. Each unit cell is separated into individual elements which are connected by nodes. As Fig. 2 shows, the hollow cylindrical tube contains a sandwich cross-section and the cross-section is divided into a number of unit cells. The configurations of unit cells in Squares, Triangles and Kagome lattice which are composed of straight lines or flat plate elements connecting the nodes or nodal lines.

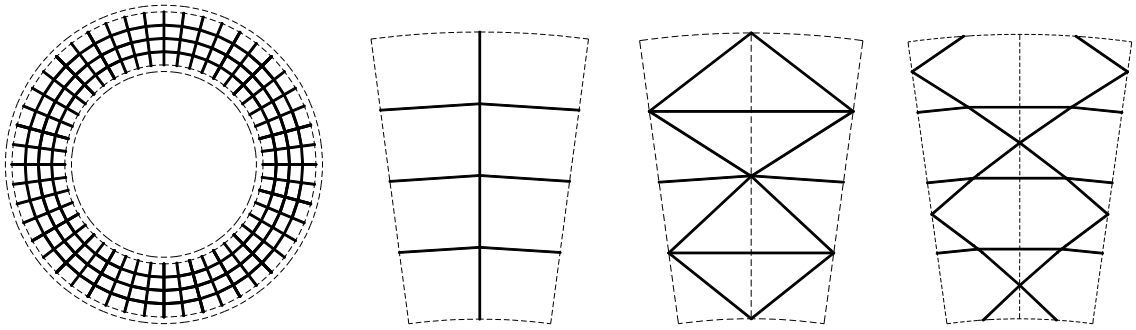

(a) Complete mode (b) Square (c) Triangle (d) Kagome

Fig. 2 Calculation models

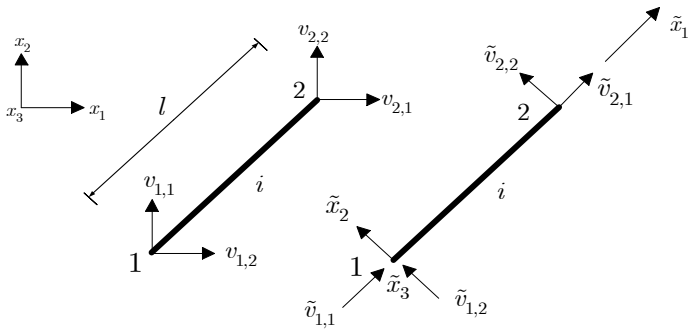

Fig. 3 Element in global and local coordinate systems

2.1 The establishment of displacement field with prismatic core

According to the illustration of Hohe (Hohe *et al*. 1999), a displacement field of each element is established for calculating the strain energy of the sandwich core. For convenience, the displacement of node i in the direction of j is denoted by $v_{i,j}$. Additionally, a local coordinate system is introduced and all quantities with respect to the local system are marked by a tilde. Hence, $\tilde{v}_{i,j}$ denotes the displacement of nodal i with respect to the x_j-direction in the local coordinate system (Fig. 3).

The whole displacement field is composed of three parts:

(1) Homogeneously distributed normal deformation in the $\tilde{x}_1 - \tilde{x}_3$ plane

$$\tilde{u}_1^{\mathrm{I}} = \tilde{v}_{1,1} + \frac{\tilde{v}_{2,1} - \tilde{v}_{1,1}}{l}\tilde{x}_1 \tag{1}$$

$$\tilde{u}_2^{\mathrm{I}} = -\frac{\nu}{1-\nu}\left(\frac{\tilde{v}_{2,1} - \tilde{v}_{1,1}}{l} + \varepsilon_{33}^{*}\right)\tilde{x}_2 = -\frac{\nu}{1-\nu}\left(\frac{\tilde{v}_{2,1} - \tilde{v}_{1,1}}{l} + \mathrm{E}_{33}\right)\tilde{x}_2 \tag{2}$$

$$\tilde{u}_3^{\mathrm{I}} = \varepsilon_{33}^{*}\tilde{x}_3 \tag{3}$$

where ε_{33}^{*} is the macroscopic strain in the x_3 direction, ν is Poisson's ratio of a cell element, and l is the length of an element in the plane of the cross section.

(2) The bending and shear deformation in the $\tilde{x}_1 - \tilde{x}_2$ plane

According to Euler-Bernoulli beam theory, the displacement of any point in the $x_1 - x_2$ plane is

$$\tilde{u}_2^{\mathrm{II}} = \frac{1}{EI}\left(C_1\tilde{x}_1^3 + C_2\tilde{x}_1^2 + C_3\tilde{x}_1 + C_4\right) \tag{4}$$

$$\tilde{u}_1^{\mathrm{II}} = -\frac{d\tilde{u}_2^2}{d\tilde{x}_1}\tilde{x}_2 = -\frac{1}{EI}\left(3C_1\tilde{x}_1^2 + 2C_2\tilde{x}_1 + C_3\right)\tilde{x}_2 \tag{5}$$

$$\tilde{u}_3^{\mathrm{II}} = 0 \tag{6}$$

where $C_1 = -2\dfrac{EI}{l^2}\left(\dfrac{\tilde{v}_{2,2} - \tilde{v}_{1,2}}{l}\right)$, $C_2 = 3\dfrac{EI}{l}\left(\dfrac{\tilde{v}_{2,2} - \tilde{v}_{1,2}}{l}\right)$, $C_3 = 0$, $C_4 = EI\tilde{v}_{1,2}$ and E is the Young's modulus of the wall cell material.

(3) Homogeneously distributed transverse shear deformation in the $\tilde{x}_1 - \tilde{x}_3$ plane

$$\tilde{u}_1^{\mathrm{III}} = \tilde{u}_2^{\mathrm{III}} = 0 \tag{7}$$

$$\tilde{u}_3^{\mathrm{III}} = \tilde{v}_{1,3} + \frac{\tilde{v}_{2,3} - \tilde{v}_{1,3}}{l}\tilde{x}_1 \tag{8}$$

The whole displacement field of an element is given by the $\tilde{u}_i = \tilde{u}_i^{\mathrm{I}} + \tilde{u}_i^{\mathrm{II}} + \tilde{u}_i^{\mathrm{III}}$. Then $\tilde{\varepsilon}_{ij}$ can be calculated by $\tilde{\varepsilon}_{ij} = \dfrac{1}{2}\left(\dfrac{\partial\tilde{u}_i}{\partial\tilde{x}_j} + \dfrac{\partial\tilde{u}_j}{\partial\tilde{x}_i}\right)$. At last, the strain vector of an element can be expressed as

$$\tilde{\varepsilon}^{*} = \left(\tilde{\varepsilon}_{11}^{*} \quad \tilde{\varepsilon}_{22}^{*} \quad \tilde{\varepsilon}_{33}^{*} \quad \tilde{\gamma}_{23}^{*} \quad \tilde{\gamma}_{13}^{*} \quad \tilde{\gamma}_{12}^{*}\right)^{\mathrm{T}} = \left(\tilde{\varepsilon}_{11} \quad \tilde{\varepsilon}_{22} \quad \tilde{\varepsilon}_{33} \quad 2\tilde{\varepsilon}_{23} \quad 2\tilde{\varepsilon}_{13} \quad 2\tilde{\varepsilon}_{12}\right)^{\mathrm{T}} \tag{9}$$

The strain energy density stored in an element can be calculated as follows

$$\begin{aligned}\tilde{U}_0^i = \frac{1}{2}\tilde{\varepsilon}^{*T}\mathbf{D}\tilde{\varepsilon}^{*} &= \frac{E\nu}{2\left(1+\nu\right)\left(1-2\nu\right)}\left(\tilde{\varepsilon}_{11} + \tilde{\varepsilon}_{22} + \tilde{\varepsilon}_{33}\right)^2 \\ &+ \frac{E}{2\left(1+\nu\right)}\left[\left(\tilde{\varepsilon}_{11}\right)^2 + \left(\tilde{\varepsilon}_{22}\right)^2 + \left(\tilde{\varepsilon}_{33}\right)^2\right] \\ &+ \frac{E}{\left(1+\nu\right)}\left[\left(\tilde{\varepsilon}_{13}\right)^2 + \left(\tilde{\varepsilon}_{23}\right)^2 + \left(\tilde{\varepsilon}_{12}\right)^2\right]\end{aligned} \tag{10}$$

where **D** is the physical matrix of the element. Therefore, the strain energy stored in the element is

$$\tilde{U}^i = \iiint_{V^i} \tilde{U}_0^i dV^i \tag{11}$$

where V^i is the volume of the element. The total strain energy stored in the unit cell with n elements can be calculated by

$$U = \sum_{i=1}^{n} \tilde{U}^i \tag{12}$$

Let the strain energy stored in the complete medium is equal to that stored in the effective medium. Then, the strain energy density of the effective medium can be calculated

$$U_0^* = \frac{1}{\Omega} U^* = \frac{1}{\Omega} U \tag{13}$$

where U^* is the strain energy density of effective medium, and Ω is the volume of the unit cell. At last, the equivalent material tensor of a representative unit cell is given by

$$C_{ijkl}^H = \frac{\partial^2 U_0^*}{\partial \varepsilon_{ij}^* \partial \varepsilon_{kl}^*} \tag{14}$$

2.2 The small strain kinematics theory and the equivalent stiffness matrix of a representative structure

According to the small strain kinematics (Liu *et al*. 2007c, Zhou *et al*. 2009), the distance between the ends of an element after deformation is approximately equal to that before deformation (Fig. 4). The relationship of them can be shown as follows

$$L\mathbf{n} = l\mathbf{F}\mathbf{n}_0 \tag{15}$$

where l is the distance between two nodes before deformation, **n** and $\mathbf{n}_0$ is the unit vector (or direction vector) of the line between two nodes, and **F** is the deformation gradient. To avoid rigid motion of the whole element, one node on an end of the element is fixed (Fig 4).

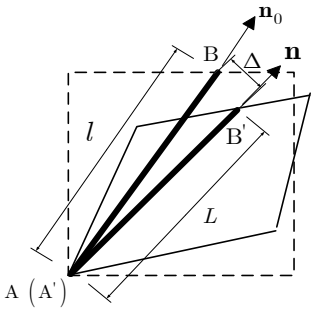

Fig. 4 Small kinematics of an element

The displacement of another node on the other end is calculated

$$\Delta = L\mathbf{n} - l\mathbf{n_0} = \left(\mathbf{F} - \mathbf{I}\right) l\mathbf{n_0} = l\mathbf{E}\mathbf{n_0} \tag{16}$$

$$\mathbf{E} = \begin{bmatrix} \mathrm{E}_{11} & \mathrm{E}_{12} & \mathrm{E}_{13} \\ & \mathrm{E}_{22} & \mathrm{E}_{23} \\ sym & & \mathrm{E}_{33} \end{bmatrix} \tag{17}$$

$$\mathbf{n_0} = \begin{pmatrix} n_{01} & n_{02} & n_{03} \end{pmatrix}^{\mathrm{T}} \tag{18}$$

The displacement can be expressed as

$$\begin{bmatrix} v_{i,1} \\ v_{i,2} \\ v_{i,3} \end{bmatrix} = \left|\mathbf{n}_{\mathbf{o}i}\right| \begin{bmatrix} \mathrm{E}_{11} & \mathrm{E}_{12} & \mathrm{E}_{13} \\ & \mathrm{E}_{22} & \mathrm{E}_{23} \\ \mathrm{sym} & & \mathrm{E}_{33} \end{bmatrix} \begin{bmatrix} n_{i,1} \\ n_{i,2} \\ n_{i,3} \end{bmatrix} \tag{19}$$

Then, the displacement in local coordinate system can be written as

$$\tilde{\mathbf{v}}_{i,j} = \mathbf{T}\mathbf{v}_{i,j} \tag{20}$$

where $\mathbf{T}$ is the transformation matrix from the global coordinate system to the local coordinate system. Then, the strain energy density of the effective medium can be calculated by Eq. (13) and the equivalent stiffness matrix of a representative unit cell is obtained by Eq. (14).

2.3 Limitations of the method in practical applications

The curved elements of a unit cell are treated as straight walls in the homogenization method used in the present paper. Unfortunately, some errors may be introduced in the calculations of this type of structures as some curved elements exist in the unit cells where the cross-section is divided by revolving periodic unit cells. If the cross-section is divided by a smaller number of unit cells, the ratio of the length of curved elements to the length of straight elements grows bigger and the curved elements cannot be replaced by straight elements as the errors could be considerable between the two models. It can be seen from Fig. 5 that there is a difference between the straight element and the curved element in the model with 24 revolving periodic unit cells. Therefore, there is a range for the number of cell elements within which this method can be applied with sufficient accuracy and finding this range is one aim of the present study, by a number of calculations using the commercial software ABAQUS.

3. The applications and discussions of this method in the homogenization of a sandwich tube

3.1 The analysis models

A series of hollow cylindrical structures with three topologies (Square, Triangle and the

Kagome) in their sandwich cross-section are analyzed through the method described above for obtaining their homogenized parameters which are assigned to EM and the static and dynamic responses and the frequencies of both CM and EM are calculated and compared. Three models of CM are shown in Fig. 6 and the material parameters of CM are given in Table 1. A series of models which contain 48, 32, 28, 24, 23, 22, 20 periodic unit cells in their sections are analyzed and the central angles of these sections are $2\pi/48$, $2\pi/32$, $2\pi/28$, $2\pi/24$, $2\pi/23$, $2\pi/22$ and $2\pi/20$ respectively. The ratios of the lengths of curved elements to the lengths of the corresponding chords are 1.000401, 1.000714, 1.001607, 1.002099, 1.002859, 1.003113, 1.003403, and 1.00412. In order to reduce the computation time, a unit of these models is selected to be analyzed with rotating periodic boundary conditions. A static pressure and a step pressure are applied to the inner side of the tube, whose magnitude is 5×10^6 Pa.

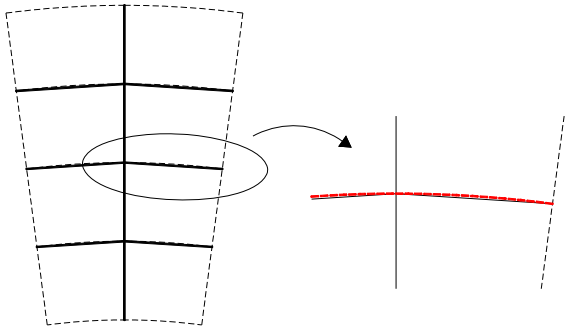

Fig. 5 Square core with 24 revolving periodic unit cells

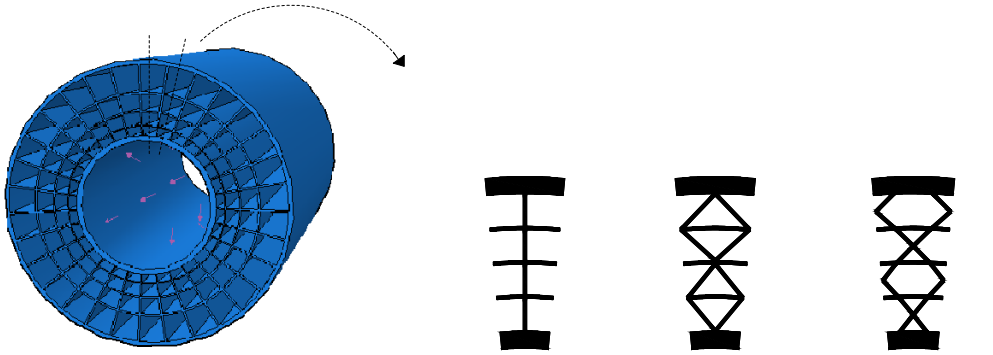

(a) the whole complete model (b) Square-32 (c)Triangle-32 (d)Kagome-32

Fig. 6 Whole complete model and the unit of the calculation models

Table 1 Parameters of materials and three topologies unit cells

E (Pa)	ρ (kg/m^3)	ν	R_{in} (m)	t (m)	h_{f} (m)	h_{c} (m)	L (m)
193×10^9	8000	0.23	0.14	0.002	0.01	0.08	1

Three regions (upper, middle and inner regions, see Fig. 7) are selected to show the results between CM and EM for comparison. The equivalent parameters of representative Kagome-32 with numbers of different unit cells are shown in Fig 8. The actual frequencies and the responses under static and step pressures of these models are obtained, and the errors between CM and EM are compared in Table 2.

3.2 The responses and errors between CM and EM under static and step pressures

The static response between CM and EM is an important indicator for indicating whether the macroscopic elasticity parameters are equivalent between two models. The static responses of the models are calculated and the errors in peak responses and strain energies between CM and EM are given in Table 2.

It can be seen that the peak responses of CM and EM agree well and the errors between the two types of models are small. The errors decrease with the increasing number of unit cells in a section, and the errors between the two types of models with the 24 unit cells in their cross-section are acceptable. The errors of models with Kagome cores are smaller than those of models with Square and Triangular cores. It is demonstrated that the homogenization method can obtain the correct homogenized parameters form CM to calculate the static responses

3.3 Errors of first five frequencies between CM and EM

The frequencies and modes are important dynamic properties of a structure. The accuracy between the frequencies of EM and those of CM directly reflects whether the dynamic characteristics of EM with the homogenized parameters obtained by the homogenization method can represent the dynamic characteristics of CM. Therefore, the first five frequencies between CM and EM are obtained and compared and the errors of frequencies between CM and EM are shown in Fig. 9.

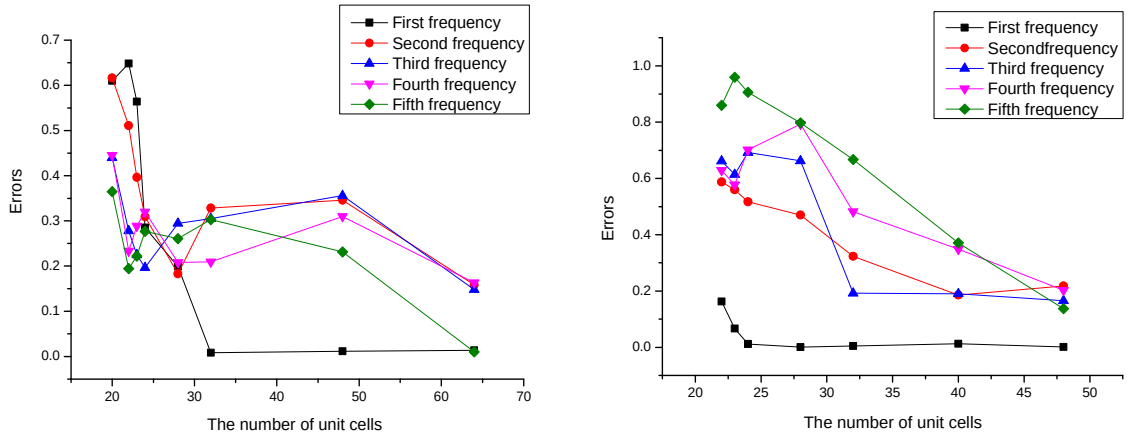

(a) Models with Square cores (b) Models with Triangular cores

Fig. 9 Errors of frequency between CM and EM

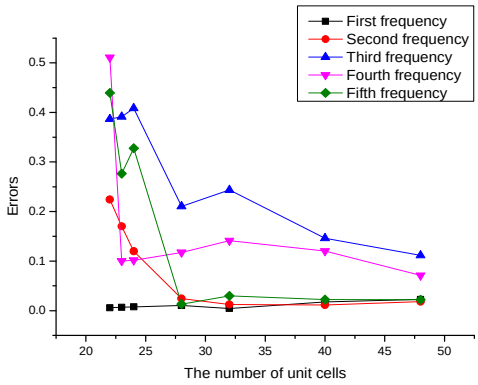

(c) Models with Kagome cores
Fig. 9 Continued

Table 2 Errors of responses between CM and EM under static pressure %

Model	Errors in displacements			Strain energy
	Inner	Middle	Upper	
Square-64	0.32	2.01	1.60	1.29
Square-48	0.02	2.85	2.39	1.99
Square-32	2.27	6.42	5.75	4.74
Square-28	8.69	9.06	12.57	11.26
Square-24	9.87	12.55	15.41	13.82
Square-23	4.31	11.47	11.94	10.58
Square-22	4.25	10.52	12.89	11.41
Square-20	3.75	9.27	14.86	13.09
Triangle-48	0.60	1.21	0.16	0.53
Triangle-32	1.27	2.47	2.14	1.60
Triangle-28	1.27	1.89	2.04	3.05
Triangle-24	2.37	2.18	5.46	4.82
Triangle-23	5.49	9.25	5.62	4.94
Triangle-22	5.30	5.22	6.00	5.32
Triangle-20	1.38	12.47	14.38	13.92
Kagome-48	0.18	0.78	0.44	0.67
Kagome-32	4.79	4.68	3.37	2.95
Kagome-28	1.86	0.20	0.09	0.02
Kagome-24	5.64	1.37	0.67	0.68
Kagome-23	7.62	1.07	0.80	0.86
Kagome-22	9.86	2.11	0.93	0.97
Kagome-20	18.32	5.38	1.34	1.45

Table 3 Errors of peak dynamic responses between CM and EM under step pressure %

Model	Errors in displacements			Kinetic energy	Strain energy
	Inner	Middle	Upper		
square-64	0.59	1.15	0.62	1.19	0.56
square-48	0.68	3.00	7.13	0.86	0.27
square-32	5.68	7.30	5.01	4.02	4.70
square-28	9.80	2.22	9.69	9.91	8.15
square-24	11.89	9.37	15.04	9.05	11.10
square-23	5.58	22.52	13.00	5.19	1.40
square-22	0.79	29.92	14.00	5.19	13.18
square-20	0.37	3.70	18.62	2.41	26.45
Triangle-48	2.99	1.27	0.24	4.13	4.95
Triangle-32	2.25	2.94	1.10	2.77	3.18
Triangle-28	2.47	4.84	0.30	4.30	6.88
Triangle-24	6.82	1.01	3.40	0.83	5.33
Triangle-23	1.29	1.36	6.20	3.94	6.85
Triangle-22	3.23	14.26	1.23	5.51	8.63
Triangle-20	8.09	9.82	5.40	6.74	10.95
Kagome-48	1.02	1.27	0.13	0.16	1.72
Kagome-32	1.10	2.42	0.76	2.27	2.39
Kagome-28	1.73	1.78	5.38	2.19	1.16
Kagome-24	2.27	4.49	2.87	4.70	3.51
Kagome-23	0.56	6.89	5.35	0.56	0.92
Kagome-22	0.63	9.22	7.66	2.40	1.71
Kagome-20	12.25	17.31	0.55	12.05	16.05

It can be seen that the frequencies of CM and EM agree very well, especially in the models with a large number of unit cells. The accuracy of the first frequency is quite higher than that of other frequencies and the accuracy of the models with Kagome cores is higher than that of models with other two topologies. It is demonstrated that the homogenization method can obtain the correct parameters and the frequencies between EM and CM agree well.

3.4 Errors of dynamic responses between CM and EM under a step pressure

As there is a successive series of blasting pressure produced in the tube when the PDE works, the dynamic responses of CM and EM under a step pressure are calculated and compared, and the errors of the peak response, kinetic energy and strain energy between the two different types of models in different regions are given in Table 3.

As Table 3 shows, the peak responses of EM agree well with the values of CM. It can be seen clearly that the errors decrease with the increasing number of unit cells in a cross-section, and the errors of models with Kagome cores are smaller than those of models with Square and Triangular

cores on the whole. The transient vibration responses and the energy of CM and EM of Kagome-48 are compared, as shown in Fig. 10. The patterns look very similar and the same types of results can also be found in other models. These results demonstrate that the method adapted in the present study can be used in the homogenization process and good results can be obtained.

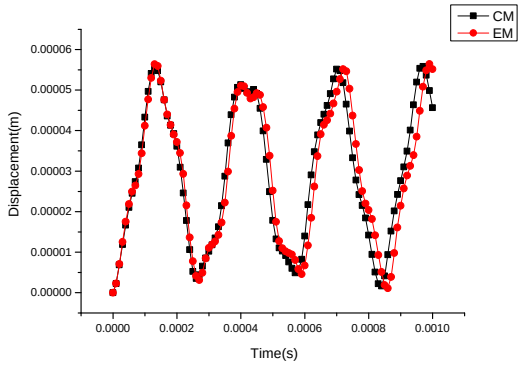

(a) Displacement of inner region

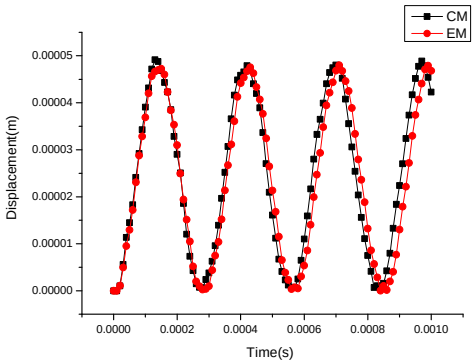

(b) Displacement of middle region

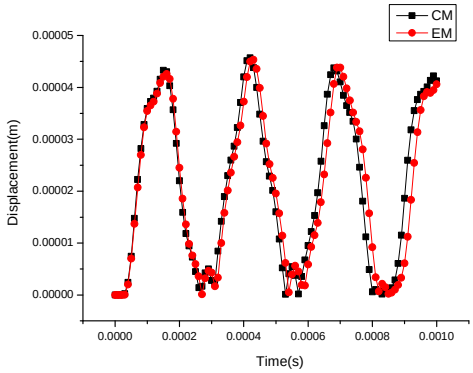

(c) Displacement of upper region

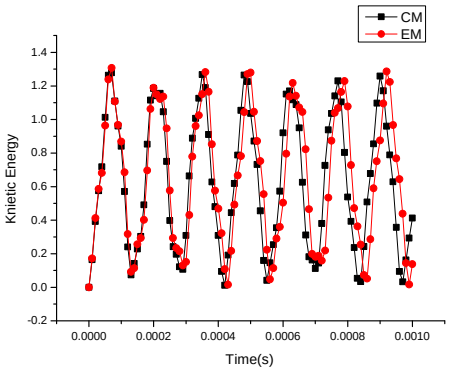

(d) Kinetic energy

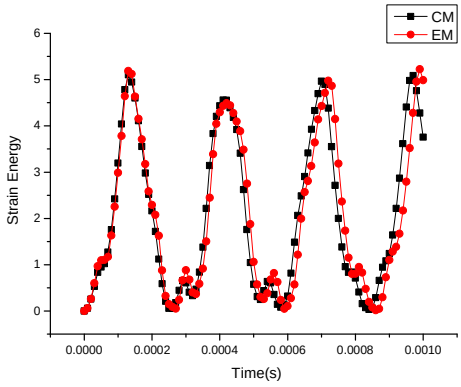

(e) Strain energy

Fig. 10 Transient vibration responses of CM and EM of Kagome-48

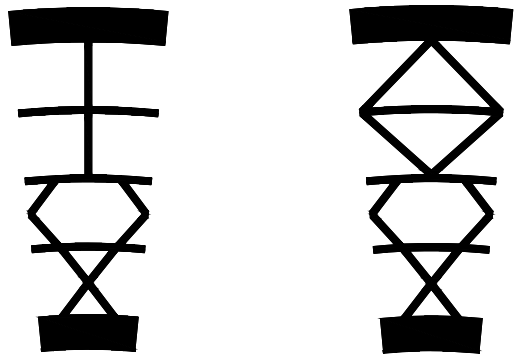

(a) Kagome-square-32 (b) Kagome-Traingle-32

Fig. 11 Multiple-topology designed sandwich tubes

Meanwhile, it should be noticed that the errors grow with the decreasing number of unit cells of the cross-section. The errors between CM and EM with 20 unit cells in a cross-section are fairly big and the results are not acceptable. After calculating and comparing the static and dynamic responses and frequencies between EMs and CMs which have the 24, 23, 22, 21 and 20 unit cells in their sections, the lower bound of the number of Square cells in a section is found to be 24, and the lower bounds of the number of Triangular and Kagome cells are found to be 22.

Generally, cellular materials have a relative density less than 0.3 (Gibson and Ashby 1997). The upper bound of the relative density is also set as 0.3 in this study. The relative density varies with the changes of the cell-wall thickness, length and the representative topology of unit cells. For example, the relative density of triangle-64 model (0.311881) and kagome-64 model (0.311906) are greater than this upper bound. After the calculations, it is found that the maximum number of unit cells in cross-sections with Square, Triangular and Kagome cores are 134, 60 and 60 and the relative densities are 0.2995, 0.2998 and 0.2998 respectively.

3.5 Effectiveness of the homogenization method on multiple-topology designed sandwich tubes

The multiple-topology designed materials studied before (Kumar and McDowell 2009) are expected to have attractive properties, such as a higher heat transfer rate and a greater loading capacity. The multiple-topology design of sandwich tube is also considered in the present paper (Fig. 11). These types of structures have different topologies in different layers, and the attractive multi-properties can be achieved by optimizing the dimensions of elements in different layers. The homogenization method is tested and verified by calculating the dynamic responses of some models shown in Fig. 11. The theoretical models are named by the topologies present in the model, for example, Kagome-Square-32 is the model shown in Fig. 11 (a).

There are two ways to treat the core of the sandwich tube, to obtain the homogenized parameters and to assign the parameters to EM. One way is to treat as a single topology and calculate the equivalent parameters for a whole model. In the second way, the core is divided into four layers as seen in Fig. 11. The first and second layer are treated as a type of topology and the third and fourth layer are treated as another type of topology, because each two layers contain a

complete unit cell of the same type of topology. The parameters are obtained from the two types of topologies and assigned to the corresponding layers of EM respectively. In order to verify the correctness and compare the differences between the two ways of obtaining parameters, the dynamic responses and energy by these two ways are calculated and the errors between CM and EM are given in Table 4 and Table 5.

Table 4 Errors between CM and EM (whole model)

Models	Errors in displacements			Kinetic energy	Strain energy
	Inner	Middle	Upper		
Square-triangle-32	8.32	12.43	5.36	4.01	12.46
Square-kagome-32	8.06	17.51	3.61	8.40	7.30
Triangle-square-32	9.35	5.51	7.47	7.50	6.60
Triangle-kagome-32	10.54	0.29	1.91	10.28	10.02
Kagome-square-32	24.93	18.30	127.10	23.32	19.67
Kagome-triangle-32	8.47	14.80	2.41	7.69	6.77

Table 5 Errors between CM and EM (two layers model)

Models	Errors in displacements			Kinetic energy	Strain energy
	Inner	Middle	Upper		
Square-triangle-32	0.06	9.64	3.49	4.87	4.20
Square-kagome-32	10.07	5.58	3.66	11.14	8.29
Triangle-square-32	0.62	13.50	2.95	2.46	5.75
Triangle-kagome-32	3.97	11.04	10.48	3.41	2.85
Kagome-square-32	11.45	12.07	7.31	9.82	5.15
Kagome-triangle-32	11.43	10.80	1.97	11.97	9.67

From the above calculations and comparisons, it is found that the errors between CM and EM defined by the second way are smaller than those of the models defined by the first way, and the second way is suitable for calculating the response of the multiple-topology designed materials. The homogenization method offers a valid way to calculate the homogenization parameters of the multiple-topology designed materials and the work on these types of materials is useful for designing the structures to obtain a better multi-physical performance.

4. Conclusions

The proposed homogenization method is able to obtain the equivalent parameters of the prismatic core efficiently. The errors in static and dynamic responses and the frequencies between CM and EM with the Square, Triangular and Kagome cores are found to be acceptable in the models with the number of the unit cells in a cross section, and the errors of models with Kagome

cores are smaller than those of models with Square and Triangular cores. The lower bound of the number of Kagome, Triangular and Square unit cells in a cross-section are 24, 22 and 22. Meanwhile, the upper bound of the number of Kagome, Triangular and Square unit cells in a cross-section are 134, 60 and 60 respectively.

The method can also be used for calculating the homogenized parameters of multiple-topology designed sandwich tubes. It is found that obtaining the parameters from separated layers and assign them to the corresponding layers is more accurate than treating the structure as a whole. The errors of peak dynamic responses between CM and EM are acceptable. It is shown through numerical simulation that the method can be used for calculating the homogenized parameters of multiple-topology designed sandwich tubes which may have attractive properties.

Acknowledgments

The authors wish to thank the National Basic Research Program of China (2011CB610300), the National Natural Science Foundation of China (10972182), the Doctoral Program Foundation of Education Ministry of China (20106102110019) and the Open Foundation of State Key Laboratory of Structural analysis of Industrial Equipment (GZ0802).

References

Cooper, M. (2004), *Impulse generation by detonation tubes,* California Institute of Technology.

Evans, A.G., Hutchinson, J.W., Fleck, N.A., Ashby, M.F. and Wadley, H.N.G. (2001), "The topological design of multifunctional cellular metals", *Progress in Materials Science*, **46**, 309-327.

Fleck, N.A., Deshpande, V.S. and Ashby, M.F. (2010), "Micro-architectured materials: past, present and future", *Proceedings of the Royal Society A: Mathematical, Physical and Engineering Science*, **466**, 2495.

Gibson, L.J. and Ashby, M.F. (1997), *Cellular Solids: Structure and Properties*, 2nd Ed., Cambridge University Press, Cambridge, U.K.

Gu, S., Lu, T. and Evans, A. (2001), "On the design of two-dimensional cellular metals for combined heat dissipation and structural load capacity", *International Journal of Heat and Mass Transfer*, **44**, 2163-2175.

Hohe, J. and Becker, W. (1999), "Effective elastic properties of triangular grid structures", *Composite Structures*, **45**, 131-145.

Hohe, J. and Becker, W. (2001), "An energetic homogenisation procedure for the elastic properties of general cellular sandwich cores", *Composites Part B: Engineering*, **32**, 185-197.

Hohe, J., Beschorner, C. and Becker, W. (1999), "Effective elastic properties of hexagonal and quadrilateral grid structures", *Composite Structures*, **46**, 73-89.

Kumar, R. and McDowell, D. (2004), "Generalized continuum modeling of 2-D periodic cellular solids", *International Journal of Solids and Structures*, **41**, 7399-7422.

Kumar, R. and McDowell, D. (2009), "Multifunctional design of two-dimensional cellular materials with tailored mesostructure", *International Journal of Solids and Structures*, **46**, 2871-2885.

Liu, T., Deng, Z. and Lu, T. (2007a), "Bi-functional optimization of actively cooled, pressurized hollow sandwich cylinders with prismatic cores", *Journal of the Mechanics and Physics of Solids*, **55**, 2565-2602.

Liu, T., Deng, Z. and Lu, T. (2007b), "Minimum weights of pressurized hollow sandwich cylinders with ultralight cellular cores", *International Journal of Solids and Structures*, **44**, 3231-3266.

Liu, T., Deng, Z. and Lu, T. (2007c), "Structural modeling of sandwich structures with lightweight cellular cores", *Acta Mech Sinica-Prc*, **23**, 545-559.

Lu, T., Valdevit, L. and Evans, A. (2005), "Active cooling by metallic sandwich structures with periodic cores", *Progress in Materials Science*, **50**, 789-815.

Ohno, N., Okumura, D. and Noguchi, H. (2002), "Microscopic symmetric bifurcation condition of cellular solids based on a homogenization theory of finite deformation", *Journal of the Mechanics and Physics of Solids*, **50**, 1125-1153.

Seepersad, C., CAllen, J., McDowell, D. and Mistree, F. (2008), "Multifunctional topology-design of cellular material structures", *J Mech Design*, **130**, 031404-031413.

Shepherd, J. (2005), *Pulse detonation engines Initiation, propagation, and performance*, California Institute of Technology, Pasadena, CA.

Valdevit, L., Hutchinson, J.W. and Evans, A.G. (2004), "Structurally optimized sandwich panels with prismatic cores", *International Journal of Solids and Structures*, **41**, 5105-5124.

Valdevit, L., Pantano, A., Stone, H. and Evans, A. (2006), "Optimal active cooling performance of metallic sandwich panels with prismatic cores", *International Journal of Heat and Mass Transfer*, **49**, 3819-3830.

Valdevit, L., Vermaak, N., Zok, F. and Evans, A.G. (2008), "A materials selection protocol for lightweight actively cooled panels", *Journal of Applied Mechanics*, **75**, 061022.

Zhou, J., Deng, Z., Liu, T. and Hou, X. (2009), "Elastic structural response of prismatic metal sandwich tubes to internal moving pressure loading", *International Journal of Solids and Structures*, **46**, 2354-2371.